Zeitschrift: Helvetica Physica Acta
Band: 41 (1968)
Heft: 6-7

Artikel: Some recent experimental studies of the gray-tin band structure
Autor: Ewald, A.W.
DOI: https://doi.org/10.5169/seals-113931

Acheson graphite in the temperature range from 13 to 300 °K. Their measurements confirm the T^2 dependence of C_V (or C_P) over the range from 13 to 54 °K even better than our previous results. At the same time KRUMHANSL and BROOKS [4] reexamined the theoretical aspects of Guerneys work and developed a more detailed theory of the vibrational modes of the graphite lattice which also leads to the T^2 dependence of the specific heat of graphite at low temperatures. In contrast to Guerney's theory, this behavior does not appear as a size effect but as an intrinsic property of the elastic anisotropy of the graphite lattice. On this basis, the experimental data from 15–1000 °K can be fitted to a theoretical curve by dividing the lattice vibrations into two types: modes with atom displacements normal to the layer planes with a Debye temperature $\theta_{D1} = 900$ °K, and modes with atom displacements within the planes with $\theta_{D2} = 2500$ °K.

The story, however, does not end here. The experimental data seem to indicate deviations from the T^2 dependence appearing below 15 °K, and the theory leaves the possibility open that at much lower temperatures a T^3 law may finally be reached. Since present-day computer facilities permit the exact numerical calculation of the vibrational spectrum of the graphite lattice, it would be very interesting to compare the results of such computations with those of new measurements at liquid helium temperatures. I am also inclined to believe that the small irradiation effect observed by us in the early measurements was due to a contribution of the relatively weakly bound interstitial atoms to the vibrational spectrum and not to a stiffening of the lattice as we assumed at that time.

References

[1] J. E. AHLBERG, I. ESTERMANN and N. O. LUNDBERG, R.S.I. *8*, 422 (1937).
[2] R. W. GUERNEY, Phys. Rev. *88*, 465 (1952).
[3] W. DE SORBO and W. W. TYLER, J. Phys. *21*, 1660 (1953).
[4] J. KRUMHANSL and H. BROOKS, J. Chem. Phys. *21*, 1663 (1952).

Some Recent Experimental Studies of the Gray-Tin Band Structure[1])

by **A. W. Ewald**
Northwestern University, Evanston, Illinois

(29. IV. 68)

Abstract. Recent studies of Shubnikov-de Haas oscillations, conventional transport, the piezo-Hall effect, magnetoflection and free-carrier absorption in gray tin are reviewed. The Shubnikov-de Haas oscillations have yielded detailed information about the Γ_8^+ conduction band including the nonparabolicity, nonsphericity and effective g-factor. The oscillations are strongly affected by the

[1]) Preparation of this review was assisted by support from the Advanced Research Projects Agency through the Northwestern Materials Research Center and from the National Science Foundation.

population of subsidiary (L_6^+) conduction band minima because of screening of the ionized impurities. Magnetoreflection measurements have permitted a direct evaluation of the $\Gamma_7^- - \Gamma_8^+$ energy separation of the inverted band structure and an assessment of the contribution of higher conduction bands to the curvature of the Γ_8^+ conduction band. Transport data obtained under suitable temperature and doping conditions have been quantitatively explained in terms of conduction in two conduction bands. The magnitudes of the stress-induced band gap and the ionization energy of stress-isolated impurity band states have been evaluated from piezo-Hall measurements. The magnitude of the $L_6^+ - \Gamma_8^+$ gap (extrapolated to $T = 0\,°\mathrm{K}$) and its temperature dependence have been evaluated from free carrier absorption measurements.

I. Introduction

A. *Historical Background*

In 1950 Professor BUSCH directed the attention of solid state physicists to the interesting semiconducting properties of gray tin [1]. The ensuing extensive investigations in his laboratory of the electrical and magnetic properties of this material stimulated similar and related work in several other places. As a result there was a considerable accumulation of experimental data when, in 1960, the review by BUSCH and KERN appeared [2]. Their compilation showed rather large discrepancies between the results of the various investigators which, it appeared, were not due to systematic experimental errors. They pointed out the need for further measurements on higher purity material and that final values could be expected only from measurements on single crystals which had just then become available [3]. It appeared, furthermore, that discrepancies in the semiconductor parameters evaluated from the data resulted in part from different methods of analysis based on different assumptions. BUSCH and KERN suggested that all analyses that had been made could by incorrect because, though they differed in other respects, they all assumed a simple two-band model. This, indeed, proved to be the case, at least for the higher temperature region in which most of the early measurements were made.

Measurements on single crystals soon yielded evidence of two types of negative carriers and therefore three-band conduction. The investigation of the symmetry properties of the magnetoresistance of *n*-type material showed a change in symmetry type between 77 and 273 °K [4]. Oscillatory magnetoresistance measurements at helium temperatures yielded an electron effective mass which was smaller by more than an order of magnitude than values estimated from high-temperature transport measurements [5]. Important clues as to the identity of the participating bands were obtained from hydrostatic pressure measurements [6]. On the basis of these experimental results and the systematic variations of energy separations in the group IV and III–V compound semiconductors, GROVES and PAUL devised their highly successful inverted band structure model [6].

B. *The Groves-Paul Band Structure Model*

The gray tin band structure model proposed by GROVES and PAUL is shown in Figure 1. This structure is qualitatively different from those of the other group IV elements and the III–V compounds. Nevertheless, it results from a systematic variation of energy separations in these semiconductors. With increasing atomic number the Γ_7^- band, which in Si and Ge lies above Γ_8^+, moves downward. In gray tin

it lies below the Γ_8^+ bands. Because of its interaction with the light-mass Γ_8^+ valence band the curvatures of both bands are reversed. The inverted Γ_8^+ light-hole band is the gray tin conduction band; the degeneracy point at Γ_8^+ is both the top of the valence

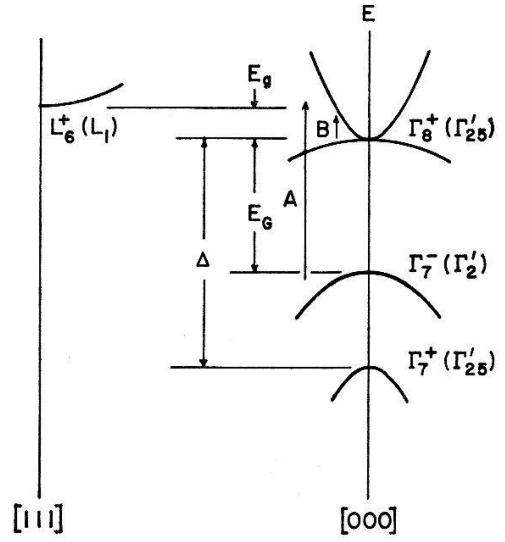

Figure 1

The Groves-Paul band structure model of gray tin. States are labeled in both the double group representation and, in parentheses, the single group representation appropriate when spin-orbit splitting is neglected. The gap between Γ_8^+ valence and conduction bands is zero. Transitions labeled A and B are observed in magnetoreflection.

band and bottom of the conduction band and the band gap is zero. This central feature of the model is not inconsistent with the repeatedly observed [2] typical semiconductor temperature dependence of the conductivity at temperatures above 160 °K. At high temperatures the L_6^+ states are sufficiently populated to dominate the transport properties which, therefore, reflect the indirect gap Eg ($\sim$ 0.1 eV). Below 77 °K these states are not populated in pure material. The Γ_8^+ electrons, because their mass is much smaller than that of the holes, dominate the transport properties. Their concentration is found to vary as $T^{3/2}$ as is expected for a zero-gap semiconductor [6].

C. *Motivation of the Recent Experiments*

The unusual qualitative features of the band structure model together with the knowledge gained from previous experiments suggested several further investigations. The success of the first Shubnikov-de Haas (SdH) measurements was due to (and established) the small effective mass of the Γ_8^+ electrons. The small energy separation between these states and the L_6^+ states and other similarities to the GaSb conduction band suggested the extension of the SdH measurements to heavily n-doped material. In the original GaSb measurements [7] the oscillations were observable only for electron concentrations greater than a critical value which is the concentration at which the L_6^+ states begin to be populated. Robinson and Rodriguez attributed the sharp increase in amplitude at the critical concentration to the screening of ionized impurities by the relatively heavy L_6^+ electrons [8]. Gray tin appeared to be a particularly suitable material for testing this theory. Further, if the oscillations could be observed at high

electron concentrations, there was the possibility of determining the energy dependence of the effective mass well into the conduction band.

The success of the first gray tin SdH measurements was also the original motivation for the search for interband magnetoreflection oscillations. After the band model was proposed, the possibility of locating the Γ_7^- valence band provided further incentive.

Recognition of the possibility of simultaneous conduction in two conduction bands suggested extensive measurements and two-band analysis of the galvanomagnetic effects under appropriate temperature and doping conditions.

Finally, the zero gap, which is the most remarkable feature of the model and is a consequence of the crystal structure symmetry, suggested the use of uniaxial stress to separate the degenerate bands. This was known to occur for the degenerate light- and heavy-mass valence bands of Si and Ge [9]. If successful in gray tin, a variety of interesting semiconductor phenomena at unusually low temperatures could be expected.

II. The Γ_8^+ Conduction Band

A. *Anisotropy*

Much of our knowledge about the Γ_8^+ conduction band has come from SdH measurements. The SdH oscillations are the result of the quantization by a magnetic field of the quasi-continuous states of this band[2]). The spacing of the quantized (Landau) levels is $\hbar\,\omega_c$ where $\omega_c = e\,B/m^*\,c$ is the cyclotron frequency. The oscillations are periodic in reciprocal magnetic field and the period[3]) P is inversely proportional to the extremal cross sectional area A of the Fermi surface which is perpendicular to the field.

$$P = 2\,\pi\,e/c\,\hbar\,A\,. \tag{1}$$

Approximately, (neglecting for the moment the nonsphericity of the band) $A \propto V^{2/3} \propto n_0^{2/3}$ where V is the k-space volume enclosed by the Fermi surface and n_0 is the Γ_8^+ electron concentration. Actually the period shows a weak orientation dependence indicating that the Fermi surface is slightly nonspherical. The shape of the Fermi surface has been determined, as described below. From it and the period measured with the field in a principal crystallographic direction n_0 may be evaluated exactly. The series of oscillatory patterns shown in Figures 2–5 illustrate the variation of period with n_0. For these samples[4]) n_0 ranges from 4×10^{15} to 7×10^{17} cm^{-3}. The total range of n_0 over which the oscillations have been observed is more than 3 orders of magnitude. Probably no other material has been studied by means of a de Haas-van Alphen-type effect over so broad a range of electron concentrations.

The shape of the Fermi surface was deduced by analyzing the angular dependence of the SdH periods and effective masses in terms of a mathematical model similar to

---

[2]) The necessary conditions for quantization are not satisfied for the highermass L_6^+ states at the magnetic fields employed in these studies.

[3]) The period is most easily evaluated through the relation $P = (1/n)\ (1/B_1 - 1/B_2)$ where B_1 locates the low-field peak n peaks away from the peak at B_2.

[4]) The lowest concentration was achieved by further purifying the highest purity commercial tin; the other samples were doped with Sb.

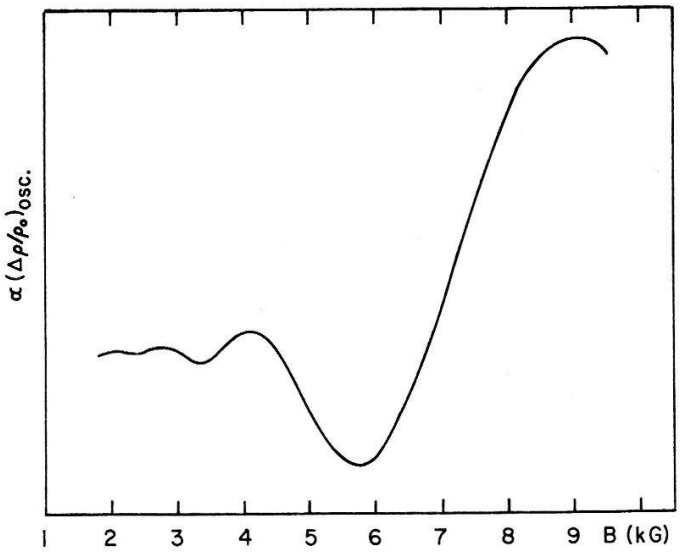

Figure 2

Oscillatory component of magnetoresistance at $T = 1.2\,°\mathrm{K}$ for a low impurity concentration; $N_d = 4.2\times 10^{15}\ \mathrm{cm}^{-3}$ (after E. D. Hinkley and A. W. Ewald, unpublished).

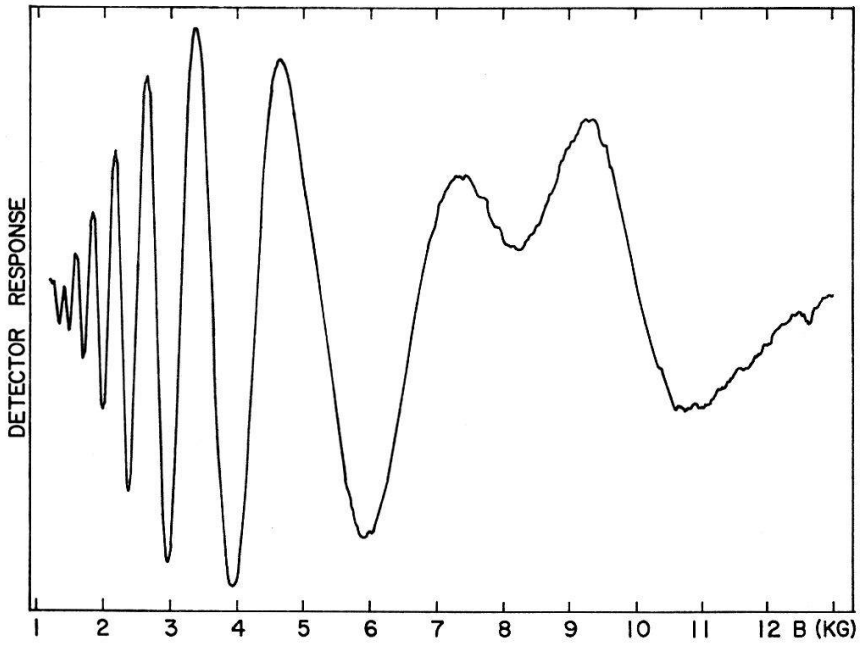

Figure 3

Magnetoresistance oscillations for $N_d = 7.6\times 10^{15}\ \mathrm{cm}^{-3}$, $P = 8.2\times 10^{-5}\ \mathrm{G}^{-1}$ and $T = 1.35\,°\mathrm{K}$. This trace and those shown in Figures 4 and 5 were obtained using field modulation and phase-sensitive detection. As in Figure 2 the oscillations begin at a relatively low field because the Dingle temperature T_D is low. The $n = 1$ Landau peak at approximately 8 kG is spin split [after B. L. Booth, Ph. D. thesis, Northwestern University (1967), (unpublished)].

that of Dresselhaus, Kip and Kittel [10] for the Γ_8^+ valence bands of Ge. According to these authors the $E(k)$ relation is

$$E = \frac{\hbar^2}{2\,m_e}\left\{A\,k_a^2 \pm \left[B^2\,k_a^4 + C^2\,(k_x^2\,k_y^2 + k_y^2\,k_z^2 + k_z^2\,k_x^2)\right]^{1/2}\right\} \tag{2}$$

where k_a is the actual k-vector to any point on the energy surfaces and A, B^2 and C^2 are coefficients to be determined experimentally. Letting $k_a^4 f(\theta,\varphi) \equiv (k_x^2\,k_y^2 + k_y^2\,k_z^2 + k_z^2\,k_x^2)$

and making approximations consistent with the smallness of the observed non-sphericity

$$E \cong \frac{\hbar^2 k_a^2}{2 m_e} \left\{ (A \pm B) \left[1 - \frac{(B+A)}{(B \pm A)} \frac{F}{2} f(\theta, \varphi) \right] \right\} \tag{3}$$

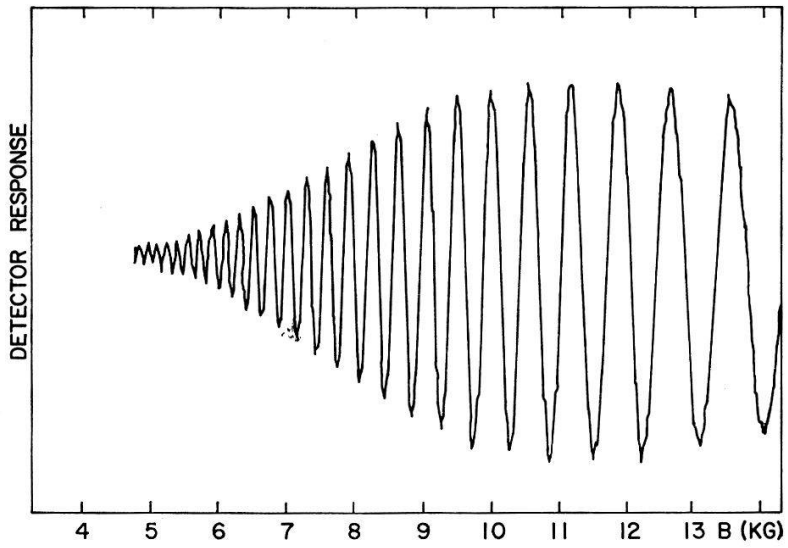

Figure 4

Oscillations for $N_d = 4 \times 10^{17}$ cm^{-3}, $P = 0.54 \times 10^{-5}$ G^{-1} and $T = 1.37$ °K. Threshold field is high and amplitude increases slowly because of high T_D [after B. L. Booth and A. W. Ewald, Phys. Rev. *168*, 796 (1968)].

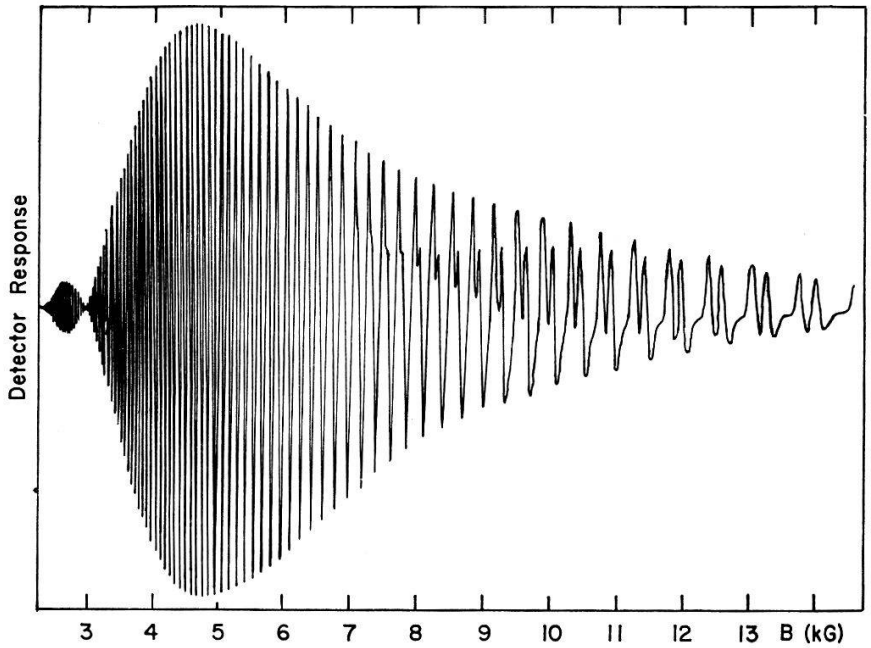

Figure 5

Oscillations for $N_d = 2.5 \times 10^{18}$ cm^{-3}, $P = 0.41 \times 10^{-5}$ G^{-1} and $T = 1.33$ °K. At this impurity concentration only a fraction of the electrons contribute directly to the oscillatory effect. The remainder ($N_d - n_0 = 1.8 \times 10^{18}$ cm^{-3}) populate high-mass L_6^+ states. The low threshold field reflects the low T_D resulting from the screening of ionized impurities by the L_6^+ electrons. Nodes and constriction of high-field amplitude are due to field modulation. Spin splitting of Landau levels is resolved above 7 kG [after B. L. Booth and A. W. Ewald, Phys. Rev. Lett. *18*, 491 (1967)].

where $F \equiv -C^2/B\,(A+B)$ and the plus and minus signs refer to the light-mass and heavy-mass Γ_8^+ bands, respectively.

To establish the applicability of this model to gray tin, BOOTH [11] derived expressions for the angular dependence of the period for the field in {100} and {110} principal planes. As an example, for the field in a {110} plane, the ratio of the period $P(\varphi)$ (measured with the field at the angle φ to a ⟨110⟩ direction) to the period $P_{\langle 111\rangle}$ (measured with the field in a ⟨111⟩ direction) is

$$\frac{P(\varphi)}{P_{\langle 111\rangle}} = \frac{A_{111}}{A(\varphi)} = 1 + \frac{(1+6\sin^2\varphi - 9\sin^4\varphi)\,F}{64} \tag{4}$$

Figure 6 shows the experimental data for several electron concentrations together with the curves calculated by adjusting the nonsphericity parameter F to fit the observed period for the [001] direction. The curves fit the data remarkably well. Although the F-values vary somewhat, the absence of a systematic variation with electron concentration is evidence that the nonsphericity is constant throughout the investigated part of the conduction band.

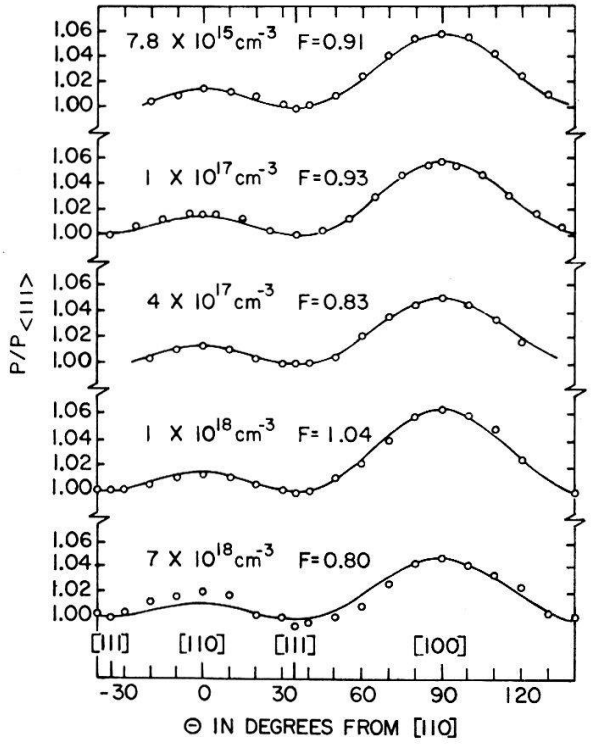

Figure 6

Angular dependence of the oscillatory period for the field in a {110} plane and several Sb concentrations. The curves were calculated using Equation (4) with F adjusted to fit the experimental data for the [100] direction [after B. L. BOOTH and A. W. EWALD, Phys. Rev. *168*, 805 (1968)].

The second method of evaluating F was through the anisotropy of the effective mass. Effective mass values for principal directions were obtained from the oscillatory amplitude as described below. These were substituted into expressions for F derived from the Dresselhaus model. The mass-determined F-values agreed with the period-determined values within the experimental uncertainty expected for a 1–2% uncertainty in the masses and periods. The average F-value for both methods and all

samples is 0.93. This may be compared with the -0.82 for the Γ_8^+ bands of Ge. The negative Ge value corresponds to $\langle 111 \rangle$ indentations on a nearly spherical Fermi surface. The positive gray-tin value produces $\langle 111 \rangle$ protrusions. This reversal reflects the inverted band structure of gray tin. Two principal cross sections of the gray-tin surface are shown in Figure 7. The (111) cross section (not shown) is circular to first order in F.

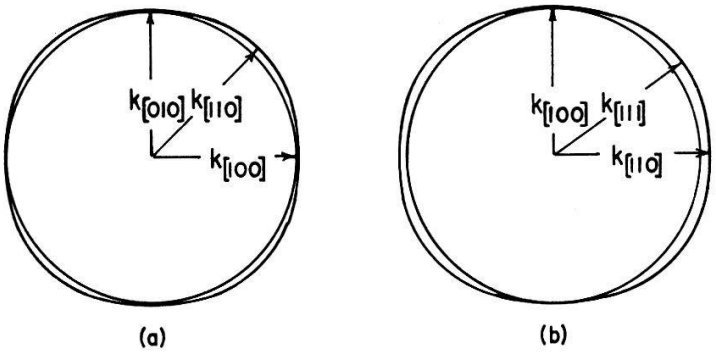

Figure 7

Principal cross sections of the Fermi surface calculated with $F = 0.93$: (a) the (001) cross section and (b) the $(1\bar{1}0)$ cross section. Circles of radius $k_{[100]}$ are inscribed for comparison. The (111) cross section (not shown) is circular to first order in the nonsphericity parameter F [after B. L. Booth and A. W. Ewald, Phys. Rev. *168*, 805 (1968)].

A more detailed comparison with Ge was made by evaluating the A, B and C^2 coefficients and, from these, the related matrix element sums characterizing the interactions between the Γ_{25}' and other bands. The matrix element sums are expected to show systematic variations among the group IV semiconductors and this was generally found to be true [11]. In particular, the sign reversal (between Ge and gray tin) of the sum for the $\Gamma_2' \, \Gamma_{25}'$ interaction confirms the inverted band structure model.

B. *Nonparabolocity*

As has been indicated, the electron effective mass, its anisotropy, and its energy dependence were obtained by studying, in the various samples, the dependence of the oscillatory amplitude upon crystal orientation, magnetic field and temperature. Under the conditions of Booth's measurements, which made use of field modulation and phasesensitive detection at twice the modulation frequency, the functional dependence of the amplitude is

$$\mathcal{A} = \frac{C \, J_2(\alpha) \, (T + T_i) \, e^{-\beta T_D m'/B}}{B^{1/2} \sinh \left[\beta \, (T + T_i) \, m'/B\right]} \tag{5}$$

where

m'	m^*/m_e = reduced effective mass
B	magnetic field
T_D	Dingle temperature
T_i	inhomogeneity temperature
β	$2\pi k_B m_e c/e\hbar = 1.468 \times 10^5$ gauss/°K
$J_2(\alpha)$	Bessel function of order 2
α	$2\pi B_M/P B^2$ where B_M is amplitude of modulated field
C	constant for a particular sample and field direction

The equivalent temperature T_D measures the broadening of the Landau levels due to scattering by ionized impurities. It is essentially the reciprocal of the lifetime of a state at the Fermi level. Similarly, T_i measures the level broadening due to sample inhomogeneity. A nonuniform impurity distribution causes variations in the band edge and, therefore, in the Landau levels. The Bessel function occurs here because of field modulation. Its effect on the oscillatory pattern is seen particularly in the low-field nodes and high-field constriction of the amplitude.

The actual data analysis in terms of Equation (5) will not be detailed here [12]. Suffice it to say that the parameters T_i, T_D and m' can be evaluated under the reasonable assumption that, at helium temperatures, T_i is temperature independent. Values of T_i for the selected samples used in this study ranged from 0.25 to 2.5 °K with the higher values occurring at the intermediate concentrations where T_D is also highest. (The behavior of T_D will be discussed below with other multiple-band effects.) The electron concentration dependence of m', i.e. the nonparabolicity of the Γ_8^+ conduction band, is shown in Figure 8 for the field in a $\langle 100 \rangle$ direction. For convenience, the reciprocal period which increases with increasing n_0 is chosen as independent variable. The linear dependence of $(m')^2$ upon $1/P$ observed at low concentrations is expected theoretically. The theory developed by KANE [13] for InSb is readily modified to take account of the inverted band structure of gray tin. When this is done, and making approximations valid for the Γ_8^+ conduction band of gray tin, the following simple relation is found.

$$(m')^2 \cong (m_0')^2 + (4.64\times10^{-8}\, m_0'\, a)/E_G\, P\,. \tag{6}$$

Here m_0' is the reduced effective mass at the band edge, $a \equiv 1 - m_0'$ and E_G is the $\Gamma_8^+ - \Gamma_7^-$ gap in eV. Thus, for a band having the Kane nonparabolicity, a plot of $(m')^2$ versus $1/P$ is linear and yields the band-edge mass and the energy gap between interacting bands. The m_0' values for principal directions range from 0.0233 to 0.0251 with an average value of 0.0243 which is in excellent agreement with the earlier result of Hinkley on higher-purity material [5]. The individual E_G values for the three principal directions differ from the average value of 0.634 eV by less than the experi-

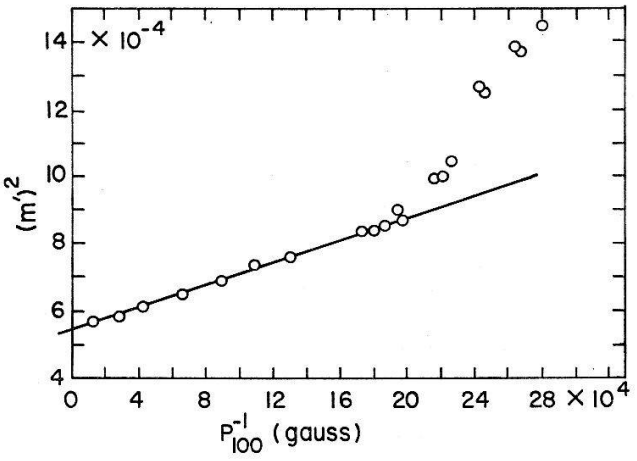

Figure 8

The square of the reduced effective mass plotted against reciprocal period for the field in a $\langle 100 \rangle$ direction. A linear dependence is expected on the basis of Kane's cubic secular equation [after B. L. BOOTH and A. W. EWALD, Phys. Rev. *168*, 796 (1968)].

mental uncertainty (1%). Knowledge of m_0' and E_G permits the evaluation of the matrix element energy defined as $E_P \equiv 2\, m_e\, P_m^2/\hbar^2$ where P_m is the momentum matrix element. For conduction electron energies much less than the spin-orbit splitting, the Kane theory gives

$$1/m_0' = 1 + (2/3)\; E_P/E_G \tag{7}$$

which yields $E_P = 39$ eV. We will comment later on these values of E_G and E_P and on the deviation of the effective mass at high electron concentrations.

The band-edge mass, the nonparabolicity, the anisotropy, and the electron concentration of the Γ_8^+ band are all involved in the exact evaluation of the Fermi level. The Fermi energy has been calculated for the entire concentration range investigated. We will indicate below how it has been used to gain information about the L_6^+ band.

C. *Spin Splitting and the Effective g-Factor*

In addition to the orbital quantization into Landau levels, the magnetic field lifts the degeneracy of the electron spin states. This may result in observable splitting of the Landau peaks of the magnetoresistance. In the recent SdH studies spin splitting was generally observed (at least at the higher fields) in samples for which $T_D < 2.5\,°\mathrm{K}$. These samples fell into two groups: those for which $N_D \leqslant 8 \times 10^{15}\ \mathrm{cm}^{-3}$ and those for which $N_D \geqslant 10^{18}\ \mathrm{cm}^{-3}$ (see Figure 12). In the low concentration sample of Figure 3 the splitting of only the $n = 1$ Landau level is well resolved. In the high-concentration sample of Figure 5 many oscillations occur above the threshold field for resolved spin splitting.

The spin-splitting data were analyzed using an expression for the Fermi surface cross section similar to one given by Ziman [14].

$$A = (n + \varphi \pm \Delta_s)\; 2\,\pi\, e\, B/c\,\hbar\,. \tag{8}$$

Here $\Delta_s = g\, m'/4$ and g is the effective spectroscopic splitting factor. The Landau level splitting, in units of $\hbar\,\omega_c$ is $2\,\Delta_s$. The phase factor φ is 1/2 for a free electron-like system and is 5/8 according to the theory of Adams and Holstein [15]. Introducing the oscillatory period through Equation (1) yields

$$n = \frac{1}{B\,P} - \varphi \mp \Delta_s\,. \tag{9}$$

Thus a plot of integers against the reciprocal field values of the split peaks should fall on two straight lines separated vertically be $2\,\Delta_s$. The many well-defined peaks of the high-concentration samples yielded essentially the same Δ_s values for the same field orientations. The angular dependence of Δ_s is similar to that of the period (see Figure 6) with values ranging between 0.16 for a ⟨100⟩ direction and about 0.1 for a ⟨111⟩ direction. This similarity suggests that the spin-splitting anisotropy, like the Fermi surface nonsphericity, is due primarily to the interaction of the higherlying Γ_{15} band with the Γ_8^+ conduction band. The g-factors for particular directions reflect the concentration dependence of m'. For the ⟨100⟩ directions they range between 28 (at low concentration) and 16, and for the ⟨111⟩ directions between 19 and 8.

III. Multiple-band Effects

A. *The Γ_8^+ and L_6^+ Conduction Bands*

As stated in the introduction, the Groves-Paul band structure model accounts for the typical semiconductor temperature dependence of the conductivity observed above 160 °K by incorporating subsidiary conduction band minima at about 0.1 eV above the Γ_8^+ degeneracy point[5]). The energy separation that had been evaluated from this temperature dependence was not very reliable, however, because the contribution to the conductivity of the high mobility Γ_8^+ electrons had been neglected. Furthermore, as is well known, this evaluation yields the energy separation extrapolated to 0 °K which, in a small gap material, may be relatively large in comparison with the actual low-temperature gap. We will now review some recent measurements of C. F. LAVINE [16] which permit a more reliable evaluation of the actual low-temperature $L_6^+ - \Gamma_8^+$ gap. These measurements also yield an estimate of the L_6^+ density-of-states effective mass.

The existence of the subsidiary minima is evidenced in several aspects of the low-temperature behavior. These states can be populated at the lowest temperatures by increasing the donor concentration N_d sufficiently or, at somewhat lower N_d values, by increasing the temperature. In either case conduction is restricted to the two conduction bands and the difficulties of analysis encountered in the higher-temperature, three-band conduction region are avoided. Figure 9 shows the helium-temperature distribution of electrons between the Γ_8^+ and L_6^+ bands as a function of N_d.

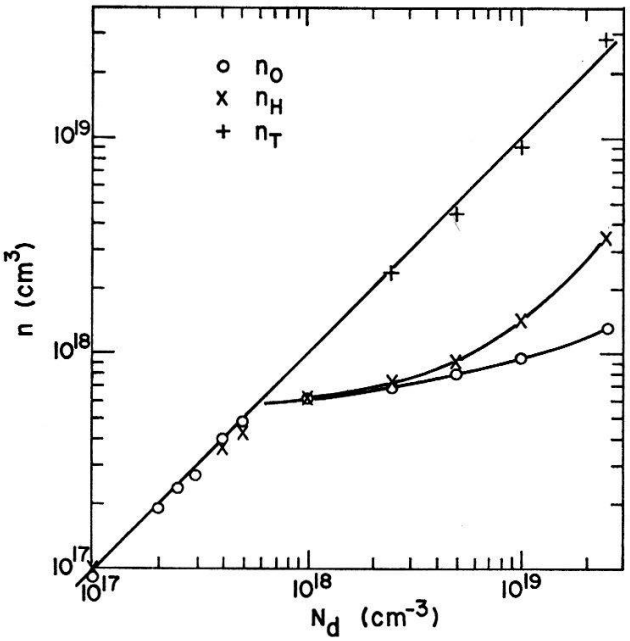

Figure 9

Electron concentrations at 4.2 °K as a function of donor concentration. The Γ_8^+ concentration n_0 was obtained from the oscillatory period; the total electron concentration n_T from the field dependence of the Hall coefficient. The equivalent concentration $n_H \equiv 1/e\,c\,R$ was obtained from the low-field Hall coefficient [after C. F. LAVINE, Ph. D. thesis, Northwestern University (1968), (unpublished)].

---

[5]) The location of these minima at the L-points of the Brillouin zone is based upon TUFTE's study of the symmetry properties of the (non-oscillatory) magnetoresistance (see Reference [4]).

In Sb-doped gray tin prepared by the phase transformation N_d is accurately predetermined by the alloy composition. The Γ_8^+ concentration n_0 was determined from the SdH period. The knee of the n_0-curve identifies the critical donor concentration N_c at which the L_6^+ states begin to be populated. The L_6^+ electron concentration n_1, is given by the difference $n_T - n_0$. Here n_T is the total electron concentration which would be measured by the high-field saturation value of the Hall coefficient ($R(\infty)$, but was actually evaluated from the field dependence of R at moderate fields. The equality of n_T and N_d establishes that added Sb donor atoms are completely ionized even at the lowest temperatures. The third curve, n_H, was obtained from the low-field Hall coefficient $R(0)$ and the relation $n_H \equiv 1/e\,c\,R(0)$. This quantity increases more rapidly than does n_0 because of the contribution to $R(0)$ of the L_6^+ electrons.

The electron concentration, n_1, is of special interest because from it and the Fermi energy evaluated in the SdH study the band-edge location and effective mass of the L_6^+ states can be evaluated. In the degenerate limit n_1 and E_F are related by

$$n_1 = \frac{1}{2\pi^2}\left(\frac{2\,m^*\,k\,T}{\hbar^2}\right)^{3/2}\frac{2}{3}\left(\frac{E_F - E_g}{k\,T}\right)^{3/2} \tag{10}$$

where the energy zero is at the bottom of the Γ_8^+ conduction band. Introducing m_{1d}, the density-of-states effective mass and $4^{2/3}$ to take account of the four L_6^+ ellipsoids, E_F is given (in eV) by

$$E_F = E_g + 3.64\times 10^{-15}\,(4^{2/3}\,m_{1d})^{-1}\,n_1^{2/3} \tag{11}$$

Figure 10 shows the linear dependence at all but the lowest n_1 values. The intersection of the straight line with the energy axis locates the band edge proper at 0.092 eV[6]). The non-zero values of $n_1^{2/3}$ at lower energies are taken as evidence of band-edge 'tail' states. The effective mass evaluated from the slope is 0.21 m_e. This represents an upper limit because the depression of the L_6^+ states due to the additional attractive potential of the ionized impurities has been neglected.

A second manifestation of the presence of the L_6^+ states is seen in the temperature dependence of the Hall coefficient of moderately doped samples. The rising coefficient with increasing temperature shown in Figure 11 is due to electron transfer from the higher-mobility Γ_8^+ states to the lower-mobility L_6^+ states. Electron transfer results from both the kT-broadening of the Fermi-level discontinuity and the lowering of the subsidiary minima with increasing temperature. The Hall data have also been used to evaluate E_g and very good agreement with the above determination was found [16], at least for samples having $N_d \geqslant 5\times 10^{17}$ cm^{-3}.

[6]) It should be noted that the agreement between the E_g evaluated here and the (0.09 ± 0.01) eV deduced from the early high-temperature conductivity measurements is more apparent than real. Different quantities are evaluated in the two measurements; the 0.092 eV is the actual low temperature gap whereas the high temperature measurements should give the value of the gap extrapolated to 0 °K with a constant (high-temperature value) of dE_g/dT. R. J. Wagner has recently evaluated the extrapolated gap and dE_g/dT through measurements of the temperature dependence of the free-carrier reflectivity minimum in the high-temperature region. Although requiring three-band analysis and the use of degenerate statistics, the method avoids the uncertainties about temperature dependences of the relaxation times. Wagner obtained a best fit to the data with an extrapolated gap of 0.11 to 0.12 eV and $dE_g/dT = 5\times 10^{-4}$ eV/°K. [R. J. Wagner, Ph. D. thesis, Northwestern University 1967, (unpublished).]

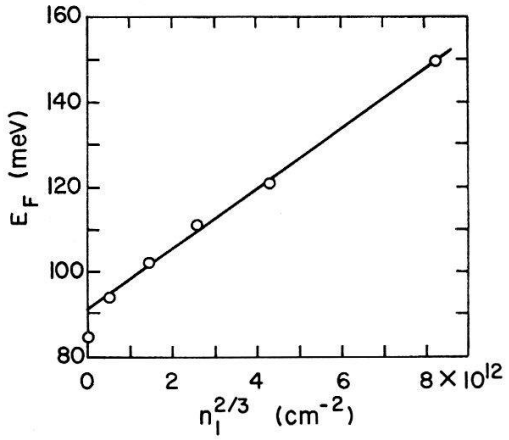

Figure 10

The Fermi energy as a function of the L_6^+ electron concentration to the 2/3 power. The intercept is E_g and the slope yields m_{1d} [after C. F. LAVINE, Ph. D. thesis, Northwestern University (1968), (unpublished)].

The discontinuous behavior at the critical concentration of two other quantities evaluated from transport measurements should be mentioned. The low-temperature mobility of the Γ_8^+ electrons at $N_d \cong 2\,N_c$ is greater (by a factor of 2) than the value extrapolated from a broad concentration region below N_c. This enhancement, beginning at $N_d = N_c$ is attributed to the screening of ionized impurities by the heavy

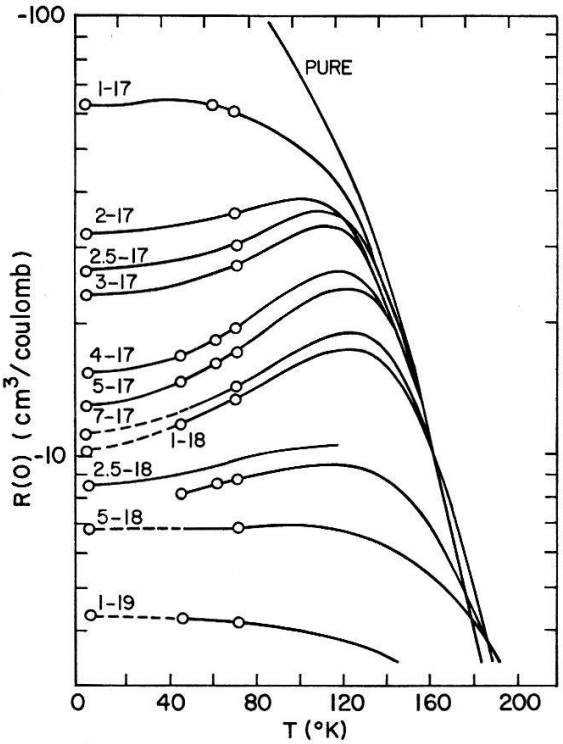

Figure 11

The temperature dependence of the low-field Hall coefficient for a series of Sb-doped samples. The notation 1–17 specifies the concentration of added Sb-atoms, 1×10^{17} cm^{-3}. The circles represent *dc* measurements used to calibrate the *ac* temperature-sweep measurements represented by the continuous curves [after C. F. LAVINE, Ph. D. thesis, Northwestern University (1968), (unpublished)].

L_6^+ electrons. There is also a marked increase in the low-temperature magnetoresistance beginning with the onset of two-band conduction.

The most dramatic effect of the population of the L_6^+ states is the indirect effect of these electrons on the amplitude of the SdH oscillations [17]. At low magnetic fields (below ~ 7 kG) the expression for the amplitude (Equation (5)) may be approximated by

$$A \cong C\, B^{1/2}\, J_2(\alpha)\, (T + T_i)\, e^{-\beta (T+T_i+T_D) m'/B}. \tag{12}$$

For given m' and B, a large amplitude requires a small effective temperature, $T + T_i + T_D$. Now as N_d is increased to populate the conduction bands, T_D also increases because of the increased number of ionized-donor scattering centers. Figure 12 shows that at $N_d = 4.7 \times 10^{17}\,\mathrm{cm}^{-3}$ T_D has reached 10 °K; it is the dominant 'temperature' limiting the amplitude. A slight increase in N_d populates L_6^+ states. These heavy electrons, according to the theory of ROBINSON and RODRIGUEZ [8], very effectively screen the ionized impurities causing the precipitous drop in T_D and an even more rapid increase in the amplitude with N_d. Comparison of the threshold field and envelope shape of Figure 4 with those of Figures 3 and 5 shows the marked effect of T_D on the amplitude. The curves of Figure 12 were calculated using the theory of Robinson and Rodriguez and two values of the dielectric constant $\varkappa$. The dashed curve is based upon the optically-determined value 23; the solid curve upon the value 20 which gives an excellent fit to the low-N_d data points.

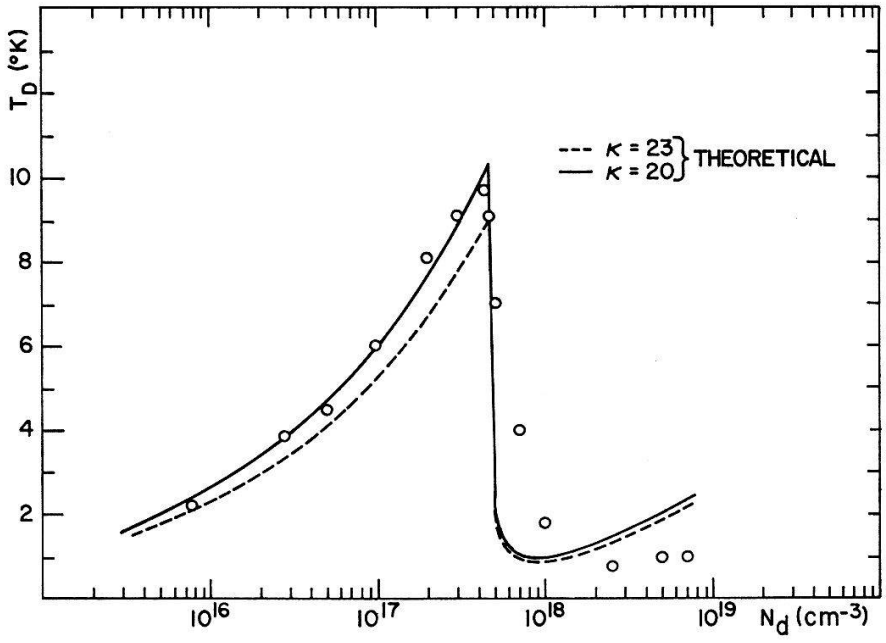

Figure 12

The Dingle temperature *vs* donor concentration. The theoretical curves were calculated for two values of the dielectric constant $\varkappa$, as explained in the text [after B. L. BOOTH and A. W. EWALD, Phys. Rev. Lett. *18*, 491 (1967)].

B. *Effects Involving the Γ_8^+ Conduction Band and the Γ_8^+ or the Γ_7^- Valence Bands*

In contrast to the studies summarized thus far, the measurements to be described in this section were made on the highest purity material. The highest purity commer-

cially available tin was further purified to reduce the donor concentration to about 5×10^{14} cm^{-3}. At this concentration intrinsic behavior is observed down to 30 °K or below depending upon the quantity under consideration. The Hall coefficient, for example, shows the $T^{3/2}$ dependence characteristic of a zero-gap semiconductor down to below 10 °K.

Of the fairly extensive results of recent conventional transport measurements on this material, one is of particular interest because it reflects the unusually simple structure of the valence band edge. By combining conductivity, Hall, and magnetoresistance data, LAVINE [16] evaluated the hole mobility shown in Figure 13. In the temperature range 30–80 °K it follows very closely the $T^{-3/2}$ dependence expected for acoustic-phonon scattering. This is in contrast with the stronger dependence invariably found in semiconductors having the typical light- and heavy-mass valence bands degenerate at $\boldsymbol{k} = 0$.

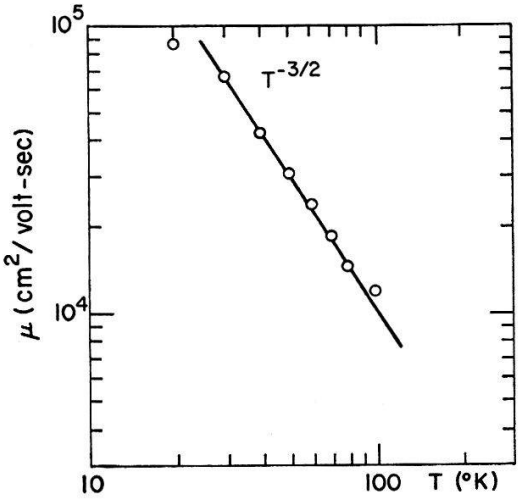

Figure 13

Temperature dependence of the hole mobility. The data shows the $T^{-3/2}$ dependence expected for acoustic-phonon scattering [after C. F. LAVINE, Ph. D. thesis, Northwestern University (1968), (unpublished)].

We consider now some current experiments undertaken by B. J. ROMAN [18] to investigate directly the most remarkable feature of the Groves-Paul model, namely, the zero band gap. It was expected that uniaxial stress would separate the degenerate Γ_8^+ bands in analogy with the effect of stress on the degenerate valence bands in Si and Ge [9]. Preliminary measurements of the conductivity under compressive stress gave encouraging results. Below 100 °K the application of stress resulted in a marked decrease in the value, and increase in the temperature coefficient, of the conductivity. It appeared that a gap on the order of 10 meV was produced by the maximum stress of 4×10^9 dynes/cm^2. Exact evaluation of so small a gap from conductivity data is difficult, however, because of the contribution of stress-induced mobility changes. To circumvent some of the difficulties, the effect of stress on the low-field Hall coefficient was investigated with the results shown in Figure 14. Intrinsic and extrinsic temperature regions are clearly distinguished. Data in the intrinsic region were used to evaluate the gap as a function of stress. This analysis was facilitated by the theoretical work of CARDONA [19] on the effect of stress on the $E(\boldsymbol{k})$ relations for the con-

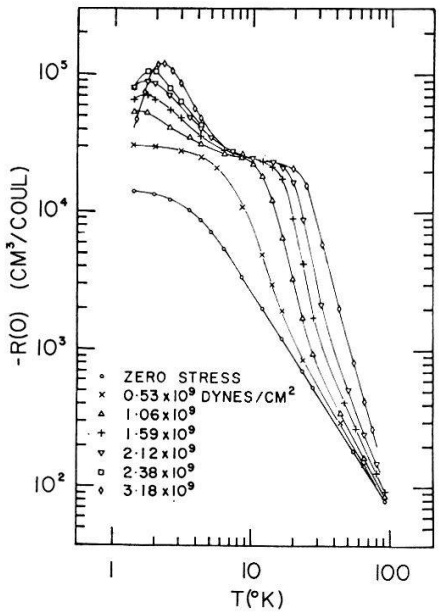

Figure 14

Temperature dependence of the low-field Hall coefficient at various uniaxial-stress values. Increasing intrinsic slope with stress reflects the splitting of the degenerate Γ_8^+ conduction and valence bands. The Hall maximum in the extrinsic region is evidence of impurity band conduction [after B. J. Roman and A. W. Ewald, Bull. Am. Phys. Soc. *13*, 408 (1968)].

duction and valence bands. Cardona showed that under [100] or [111] stress both bands become highly anisotropic and nonparabolic near $\boldsymbol{k} = 0$. In particular, the valence band maximum is shifted away from $\boldsymbol{k} = 0$ in directions transverse to the stress axis. The thermal gap therefore becomes an indirect gap and is estimated to be only one-half the direct gap at $\boldsymbol{k} = 0$. From the stress-modified $E(\boldsymbol{k})$ expressions Roman derived expressions for the densities of states which were then used in place of the usual spherical and parabolic band expressions in analyzing the Hall data. The stress dependence of the thermal gap is shown in Figure 15.

In the extrinsic region below about 15 °K the Hall coefficient shows an unexpected and interesting behavior. All but the lowest stress-value curves show a temperature

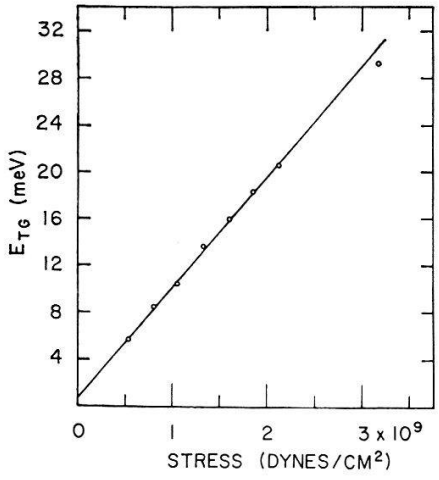

Figure 15

The thermal gap between Γ_8^+ conduction and valence bands as a function of uniaxial stress [after B. J. Roman and A. W. Ewald, Bull. Am. Phys. Soc. *13*, 408 (1968)].

and stress independent region. This is the exhaustion region. At lower temperatures the Hall coefficient passes through a maximum characteristic of impurity band conduction. In contrast to InSb, there is here a discrete impurity band even at the very low fields ($\sim$ 100 G) used in the Hall measurements. Using the exhaustion-range and maximum values of the Hall coefficient, the location of the maximum, and conduction band parameters from the SdH study, the ionization energy ε_d has been evaluated. For those Hall curves which show a definite maximum ε_d lies between 0.3 and 1.0 meV and is directly proportional to the stress. The latter strongly suggests that in unstrained gray tin (of even the highest purity) $\varepsilon_d = 0$ which, in light of the zero gap, seems intuitively reasonable.

Finally, we will briefly summarize the recently reported results of interband magnetoreflection measurements [20]. Two sets of magneto-optical transitions have been observed. The first, represented by arrow A in Figure 1, are from filled Landau levels in the Γ_7^- valence band to empty levels in the Γ_8^+ conduction band. The second, denoted by arrow B, takes place between the Γ_8^+ valence and conduction bands. Figure 16 shows the magnetoreflection traces made by sweeping the magnetic field at fixed photon energies. The peaks of the $\Gamma_8^+ \rightarrow \Gamma_8^+$ transitions at 0.23 eV resemble the idealized magnetoreflectivity form with sharp low-field edges and high-field tails [21]. The trace at 0.43 eV shows closely space $\Gamma_8^+ \rightarrow \Gamma_8^+$ transitions superimposed upon a broad peak caused by a $\Gamma_7^- \rightarrow \Gamma_8^+$ transition. Similar traces have been obtained at other photon energies covering the range 0.05–0.55 eV for the $\Gamma_8^+ \rightarrow \Gamma_8^+$ transitions and the range 0.425–0.55 eV for the $\Gamma_7^- \rightarrow \Gamma_8^+$ transitions. Plots of photon energy against resonance fields (taken at the magnetoreflection maxima) are qualitatively similar to those recently reported [22] for HgTe, which is another inverted band structure semiconductor. The fitting of the experimental data with theoretical curves

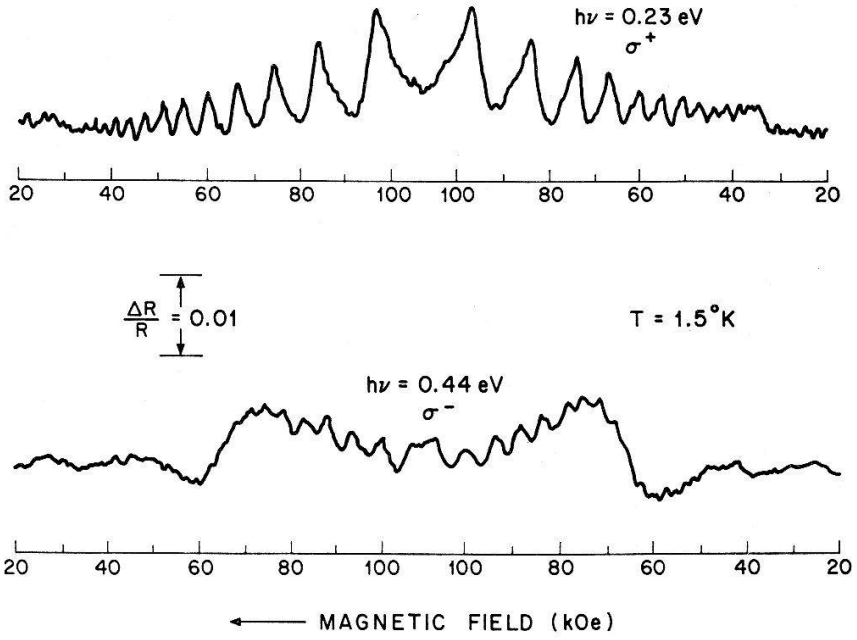

Figure 16

Traces of magnetoreflection made by sweeping the magnetic field at fixed photon energies. Upper trace shows peaks due to $\Gamma_8^+ \rightarrow \Gamma_8^+$ transitions and lower trace shows small peaks from these transitions superimposed on a large $\Gamma_7^- \rightarrow \Gamma_8^+$ peak [after S. H. Groves, C. R. Pidgeon, A. W. Ewald and R. J. Wagner, Bull. Am. Phys. Soc. *13*, 429 (1968)].

is now in progress. The method employed was developed by PIDGEON and BROWN [23] in their analysis of the InSb magnetoabsorption and has also been applied to HgTe magnetoreflection data by GROVES et al. [22]. A preliminary fit to the gray tin data is obtained for $E_G = 0.41$ eV and $E_P = 29$ eV. This more directly determined value of E_G is considerably smaller than the value deduced from the nonparabolicity of the conduction band. The analysis of the SdH data was based on Kane's cubic secular equation which does not include the effects of higher bands (Γ_{12} and Γ_{15}). It now appears that these effects cannot be neglected even for the lower portion of the conduction band [where the (m'^2) dependence on $1/P$ is linear] and, further, that they may be responsible for the deviation from linearity at high electron concentrations. Effective mass values calculated using the E_G and E_P quoted above together with the present best estimates of the higher band parameters are in good agreement with the SdH values for concentrations up to 5×10^{17} cm^{-3}.

IV. Concluding Remarks

Space has not permitted a comprehensive review of all of the recent experimental studies of gray tin. This summary of selected experiments should, however, indicate the type of information that is being obtained and how well it is correlated through the Groves-Paul model. Our knowledge of some parts of the band structure is as complete as for the most thoroughly studied semiconductors. This is true of the Γ_8^+ conduction band. There are also reasonably reliable determinations of the density-of-states effective masses of L_6^+ electrons and Γ_8^+ holes, the latter obtained from free carrier reflectivity measurements [24]. Direct experimental information on the anisotropy of these bands would be desirable.

Though this summary has emphasized the evaluation of band parameters, other aspects of the results are of equal interest and may be of greater significance relative to future experiments. The large amplitude SdH oscillations observable over broad donor and electron concentration ranges can be further exploited. An investigation of the specific donor dependence of the ionized impurity screening, for example, should be interesting. The existence of an isolated impurity band in the stress-induced gap suggests further experiments on higher purity material and at higher magnetic fields and lower temperatures.

Other areas for future experiments are suggested by two recent theoretical developments. LIU and BRUST [25] have shown that, because of the specific symmetry of the wave functions at the point of contact between the conduction and valence bands, the wave-number dependent dielectric function $\varepsilon(q)$ has a singularity of the form $1/q$ in the long wavelength limit. This, they reason, should result in a donor-concentration dependent electron mobility at low temperatures where ionized impurity scattering dominates. Such an effect has been observed in relatively pure specimens [16]. Further dielectric constant measurements should be of interest. The second theoretical development is the prediction that gray tin may, under suitable conditions, become electronically unstable and undergo a transition to an excitonic state. KOHN and SHERRINGTON [26] have estimated that this may occur in samples of sufficient purity ($N_d \leqslant 10^{14}$ cm^{-3}) at about 3 °K. The observation of this type of phase transition would certainly stimulate a number of experiments. In any event, it

appears that gray tin will continue to be of considerable interest, both theoretically and experimentally.

Acknowledgments

The author expresses his gratitude to S. H. GROVES, C. R. PIDGEON and R. J. WAGNER for the use of Figure 16 before its publication elsewhere, and to E. D. HINKLEY, B. L. BOOTH, R. J. WAGNER, C. F. LAVINE and B. J. ROMAN for the use of results contained in their respective theses, some of which have not yet appeared elsewhere in the literature.

References

[1] G. A. BUSCH, J. WIELAND and H. ZOLLER, Helv. phys. Acta *23*, 528 (1950).
[2] G. A. BUSCH and R. KERN, *Solid State Physics*, edited by F. Seitz and D. Turnbull (Academic Press, New York 1960) *11*, p. 1.
[3] A. W. EWALD and O. N. TUFTE, J. appl. Phys. *29*, 1007 (1958).
[4] O. N. TUFTE and A. W. EWALD, Phys. Rev. *122*, 1431 (1961).
[5] E. D. HINKLEY and A. W. EWALD, Phys. Rev. *134*, A1261 (1964).
[6] S. H. GROVES and W. PAUL, Phys. Rev. Lett. *11*, 194 (1963); *Proceedings of the Seventh International Conference on the Physics of Semiconductors, Paris 1964* (Dunod Cie., Paris 1964), p. 41.
[7] W. M. BECKER and H. Y. FAN, in *Proceedings of the Seventh International Conference on the Physics of Semiconductors, Paris 1964* (Dunod Cie., Paris 1964), p. 663.
[8] J. E. ROBINSON and S. RODRIGUEZ, Phys. Rev. *135*, A779 (1964).
[9] J. C. HENSEL and G. FEHER, Phys. Rev. *129*, 1041 (1963).
[10] G. DRESSELHAUS, A. F. KIP and C. KITTEL, Phys. Rev. *98*, 368 (1955).
[11] B. L. BOOTH, Ph. D. thesis, Northwestern University (1957), (unpublished); B. L. BOOTH and A. W. EWALD, Phys. Rev. *168*, 805 (1968).
[12] B. L. BOOTH and A. W. EWALD, Phys. Rev. *168*, 796 (1968).
[13] E. O. KANE, J. Phys. Chem. Solids *1*, 249 (1957).
[14] J. M. ZIMAN, *Electrons and Phonons* (Oxford University Press, London 1960), p. 523.
[15] E. N. ADAMS and T. D. HOLSTEIN, J. Phys. Chem. Solids *10*, 254 (1959).
[16] C. F. LAVINE and A. W. EWALD, Bull. Am. Phys. Soc. *11*, 847 (1966); C. F. LAVINE, Ph. D. thesis, Northwestern University (1968), (unpublished).
[17] B. L. BOOTH and A. W. EWALD, Phys. Rev. Lett. *18*, 491 (1967).
[18] B. J. ROMAN and A. W. EWALD, Bull. Am. Phys. Soc. *13*, 408 (1968).
[19] M. CARDONA, Solid St. Commun. *5*, 233 (1967).
[20] S. H. GROVES, C. R. PIDGEON, A. W. EWALD and R. J. WAGNER, Bull. Am. Phys. Soc. *13*, 429 (1968).
[21] M. S. DRESSELHAUS and G. DRESSELHAUS, Phys. Rev. *125*, 499 (1962).
[22] S. H. GROVES, R. N. BROWN and C. R. PIDGEON, Phys. Rev. *161*, 779 (1967).
[23] C. R. PIDGEON and R. N. BROWN, Phys. Rev. *146*, 575 (1966).
[24] R. J. WAGNER and A. W. EWALD, Bull. Am. Phys. Soc. *11*, 828 (1966); R. J. WAGNER, Ph. D. thesis, Northwestern University (1967), (unpublished).
[25] L. LIU and D. BRUST, Phys. Rev. Lett. *20*, 651 (1968).
[26] W. KOHN and D. SHERRINGTON, Bull. Am. Phys. Soc. *13*, 377 (1968).